

# Analysis of DGS Filters using $\pi$ Circuit Model

Sambhav Malhotra<sup>1</sup> and Mohammad Hashmi<sup>2</sup>

<sup>1</sup>Indraprastha Institute of Information Technology Delhi

<sup>2</sup>Indraprastha Institute of Information Technology

May 5, 2020

## Abstract

Two filters using Defected Ground Structures have been proposed. First, a multiple frequency band stop filter utilizing a semi-H defect in the ground plane is presented. This structure is then prototyped on a Rogers 4350B substrate of overall size 45 mm  $\times$  15 mm, and external SMD capacitors have been employed to control the resonance of the circuit, for the stopband frequencies of 433 MHz, 700 MHz and 915 MHz. An equivalent circuit is also proposed for this multi-band design. The second filter is a combination of a band-stop and band-pass filter in one structure. The filter, operating with a controllable passband and stopband frequency is fabricated, on Rogers 4350B lossy substrate, to validate the EM and circuit simulation results. Two SMD capacitors have been loaded in the filter to control the pass band and stop band frequencies of the filter with a structure size of 20 mm  $\times$  20 mm. Furthermore, a novel equivalent circuit model encompassing the band-pass and band-stop frequency response of the DGS based filter is proposed.

## Section I: Introduction

Defected Ground Structures (DGS) were introduced as an alternative method to improve the performance of microstrip circuits and components while minimizing the overall size of the design[1]. In this structure, defects are introduced in ground plane to improve the frequency response of the considered components. The geometry of this defect is selected such that it disturbs the surface current in the ground plane and helps in achieving the desired electromagnetic effects.

Many DGS based band-stop filters have been reported in literature that are modelled through equivalent parallel LC or RLC circuits[2,3]. There have been subsequent reports of advancements and improvements in the representation of equivalent LC or RLC circuits[4-6]. These equivalent circuit models look at the resonant frequency and model the dielectric losses in the form of a resistance and provide simpler ways to understand and verify performances through EM simulation results. However, this approach does not consider the effects of the discontinuity present between the microstrip line and the defected ground. The report on  $\pi$ - type equivalent circuit to model the DGS looks into this concern to some extent[7]. Here, the series element is a classic LC resonator which controls the resonant frequency of the circuit. The parallel RC modules in the model accounts for the fringing fields and its associated losses. The work does not explore the use of external capacitors in tuning the frequency. Furthermore, the design presented is disadvantageous at lower frequencies because frequency is controlled only by the shape of the defect. It requires an increase in inductance and this effectively leads to increased size of the DGS.

In this letter, two different DGS structures have been explored and analyzed. First is an arbitrary multi-band DGS based band stop filter using semi-H DGS and its equivalent circuit model. It improves on the existing  $\pi$  circuit model and proposes an approach to accommodate multiple bands. The second work focuses on the design of a passband and stopband frequency design using an H-shaped DGS. In both cases, the presence of

external SMD capacitor provides control over the achievable resonant frequency, enables good narrowband response, and reduces the size of the overall structure. Furthermore, changing the shape of the DGS acts as a second controller of the resonant frequency for both structures. Section II and III focus on the design and prototype authentication of the multi-band BSF system. Section IV, V and VI improve on the band-stop filter circuit model and introduce a band-pass frequency response to the original system

## Section II: Theoretical Analysis

### Design of Tri-Band DGS BSF filter

To demonstrate the proposed technique, a semi-H shaped DGS with three different defects in the ground plane with all the marked parameters, Fig. 1, is considered. Its top plane with marked parameters is depicted in Fig. 2.

Fig.1-> Defected Ground Plane with 3 different sizes, which represent 3 different frequencies

Fig.2-> Top plane with a 50 Microstrip Line(MSL)

Table I: Parameters for DGS Filter Design

This architecture effectively translates to three distinct band-stop frequencies for the filter. A thorough simulation and optimization in CST environment is carried out and the resulting parameters are given in Table I. It is imperative to note that the three chosen frequencies in this study are 433 MHz, 700 MHz, and 915 MHz and the resonance in EM simulation is optimized accordingly. Furthermore, three SMD capacitors need to be loaded in the respective excitation slots for synthesis of resonances at the chosen frequencies as well as for improvements of the overall quality factor and their values are also included in Table I.

### $\pi$ type Εχνιαλεντ ἰρσυιτ Μοδελ

In order to understand the working of the DGS based filter, firstly a single band  $\pi$ -type circuit model is developed, using an earlier approach[7], as shown in Fig. 3. The inductor and capacitor in parallel represent the resonant frequency of the circuit. In this work, the resistors are introduced to model dielectric losses. The parallel RC circuit models the fringing fields at the discontinuity between the transmission line and DGS. An earlier technique requires all the ABCD parameters to calculate the resistances, capacitances, and inductance of this equivalent circuit, whereas we propose a simpler approach in which a less rigorous computation enables the derivation of all the relevant parameters of the equivalent circuit. For example, first, the CST simulation and optimization determines the value of SMD capacitor for any specified resonant frequency. This can then be used for the computation of the inductance and resistance of the equivalent circuit using (1). Furthermore, the calculation of the parallel RC modules can be done from just two of the ABCD parameters(2)-(3).

Fig.3-> Pi-Type Circuit model for single band system

$$R = \text{Real}(Z_{11}), L = \frac{1}{4 * \pi^2 * f^2 * C_{\text{SMD}}} \quad (1)$$

$$A = \frac{[(1+S_{11})*(1-S_{11})] + S_{21}^2}{2 * S_{21}} \quad (2)$$

$$B = \frac{[(1+S_{11})*(1+S_{11}) - S_{21}^2]}{2 * S_{21}} \quad (3)$$

$$Y_b = \frac{A-1}{B}, C_p = \frac{\text{Imaginary}(Y_b)}{2*\pi*f}, R_p = \frac{1}{\text{Real}(Y_b)} \quad (4)$$

Fig.4 -> EM and Circuit Simulation at 915 MHz

Table II: Parameters for Single Band Circuit Model

The efficacy of the equivalent circuit is evaluated by simulating it at 915 MHz in the Keysight ADS environment. A good agreement between the circuit and EM simulation results, depicted in Fig. 4, is obtained for the optimized equivalent circuit parameters given in Table II. Here, the parameters for the single band EM simulation is taken from Table I. In brief, a good agreement provides the requisite confidence that this circuit model can be readily used for the development of multi-band equivalent circuit. An important point to note is that the capacitance affects the resonant frequency more significantly than inductance or the size of the DGS. Therefore, keeping that in perspective, the resonant frequency is controlled with the help of external SMD during design stage while the inductance plays the role of secondary controller of the resonant frequency.

### Μulti band π type Εχιαλεντ ἰρσυιτ Μοδελ

Now, to utilize the single band concept in the design of multi-band circuit, a flowchart, depicted in Fig. 5, is developed. In essence, the single-band circuit model is cascaded multiple times to meet the requirements. For demonstration of the proposed concept, a tri-band band-stop filter is developed as shown in Fig. 6 to obtain three distinct band-stop frequency responses at the frequencies of 433 MHz, 700 MHz, and 915 MHz. The simulations were carried out at both the structure and circuit levels and the resulting optimized circuit level parameters are given in Table III. Optimization of the structure is done to ensure that the three cascaded sections largely work independently of each other and this situation is observed in the respective surface current distributions. The apparent excellent agreement between the EM and circuit simulation results, in Fig. 7, provide a solid ground for confidence in the developed circuit model.

Fig.5 -> Flow chart depicting the multi-band stop band filter design process

Fig.6-> Cascaded Tri-Band Filter using π type circuit model

Fig.7-> Tri band EM and Circuit Simulation Results.

Table III:Parameters for Sections 2 and 3 of π type model

### Section III: Measurement and Results

A BSF prototype using the proposed concept is developed on Rogers 4350B substrate. The BSF is connected by two ports, both connected to the defected ground and also to the 50 Ω microstrip line as shown in Figs. 8 and 9. The external SMD capacitors are soldered on the excitation slots of the semi-H shaped DGS. The S-parameters are then measured using Keysight E5063A VNA over a frequency range of 0.4 to 0.95 GHz. The measured results are plotted in Fig. 10 and apparently there are three clear resonant frequencies. The

measured result is in agreement with the circuit simulation and EM simulation results given in Fig. 7 and therefore validate the tri-band filter design technique.

Fig.8 -> Fabricated Ground Plane of the DGS showing Semi-H Defect

Fig.9-> Fabricated Top Plane of the DGS showing microstrip feed line and ports.

Fig.10-> Measured Results of the Multi-band DGS filter

It can be seen that slight shift in frequencies has taken place and this can be attributed to the presence of the external SMD capacitors. These SMD capacitors help in size reduction and are relatively easy to solder but suffer from poor tolerances. It has been observed that tolerances of even [?] 0.25 pF can cause significant shift in the resonant frequency. In brief, the shifting of resonant frequencies can be overcome by using lower tolerance capacitors. Furthermore, the rejection in the measured values at the three frequencies is different when compared to the EM and circuit simulation values due to the port,solder and connector losses.

#### Section IV: New DGS Filter

Communication systems require not only band-stop frequencies but band-pass frequencies for efficient communication. To understand band-stop and band-pass characteristics of a DGS filter system, an H-shaped DGS has been presented. The defect in the ground plane is shown in Fig. 11. This defect in the ground plane perturbs the 50  $\Omega$  microstrip transmission line on the top plane to give rise to a stop-band frequency as done earlier, with the semi-h defect. After designing the initial band-stop filter, we introduce a gap in the 50 $\Omega$  microstrip feed line in the top plane. Another SMD capacitor is mounted in that gap, which allows the control of the pass band resonant frequency. The top plane view is depicted in Fig. 12. All the marked parameters to help replicate the work done is given in Table IV.

Figure 11: Ground plane with H-shaped DGS

Figure 12: Top plane with a 50  $\Omega$  feed line and a coupling gap

Table IV: Parameters for Band-Pass Filter Design

#### Section V: Improved Circuit Model

The equivalent inductance along with the coupling gap capacitance present in the microstrip feed line introduces a series resonance and hence an additional frequency response to the circuit. This additional frequency is the passband. The introduction of a series capacitor to the original circuit, shown in Fig. 13, includes the modules responsible for the series and parallel resonances. Furthermore, the parallel RC combination used to model the fringing effects remain as part of the circuit and no further changes are made in the original circuit. The circuit parameters obtained using (5) and (6) are provided in Table V.

$$L_{\text{bandpass}} = \frac{L_{\text{bandstop}}}{1 - \left(\frac{f_{\text{bandpass}}}{f_{\text{bandstop}}}\right)^2} (5) C_{\text{bandpass}} = \frac{25.33}{L_{\text{bandpass}} * f_{\text{bandpass}}^2} (6)$$

Moreover, the choice of the stop band and passband frequencies has to be in a manner such that  $f_{\text{bandpass}} < f_{\text{bandstop}}$ . An example simulation was carried out by considering 0.70 GHz as the passband frequency and 0.77 as the stop-band frequency and the corresponding EM simulation and circuit simulation results are depicted in Fig. 14. The results clearly demonstrate the effectiveness of the proposed equivalent circuit that models both the bandpass and bandstop behavior.

Figure 13-  $\pi$  type circuit model for bandpass/bandstop filter

Figure 14-EM and circuit simulation of passband and stopband frequencies

Table V: Parameters for New Circuit Model

#### Section VI: Measured Results for the New DGS

Fig.15- Ground Plane view of fabricated Bandpass/bandstop filter

Fig.16- Top Plane view of fabricated prototype

Fig. 17- Measured result showing the Passband and Stopband Frequencies.

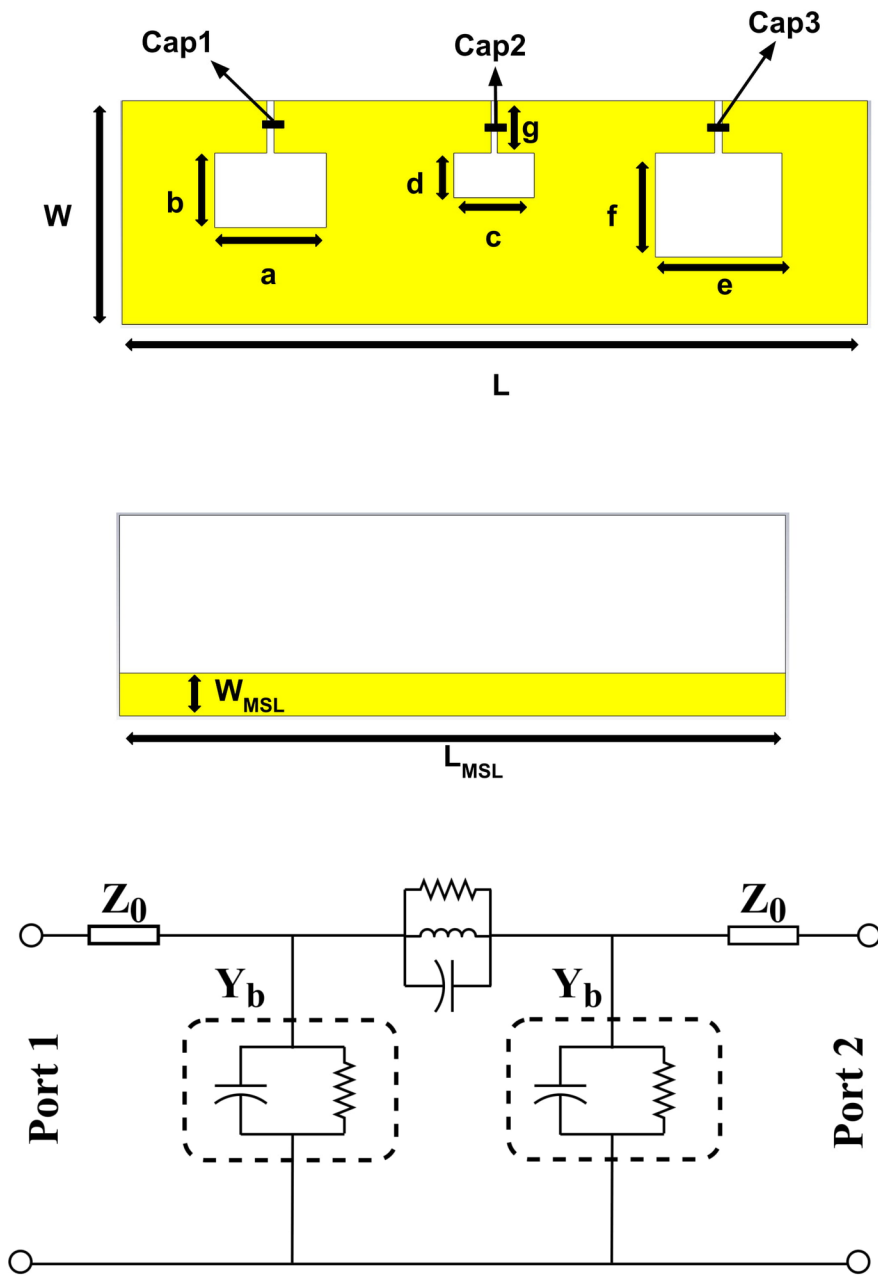
The band-pass filter is designed in CST Microwave Studio and fabricated on a Rogers 4350B substrate having  $\epsilon_r = 3.66$ , height of 1.52 mm and a loss tangent of 0.0037. The fabrication is shown in Fig. 15 and 16, which shows the top and the ground plane of the structure. The 9 pF capacitor is soldered onto the gap in the DGS and the 3 pF capacitor is mounted in the coupling gap in the 50  $\Omega$  microstrip line. Two SMA connectors with impedance 50  $\Omega$  are also soldered and the filter is measured using a Keysight N9926A handheld VNA. The result for the fabricated structure, given in Fig. 17, clearly shows the presence of a sharp band-stop and band-pass response. Similar to the previous design, the work proposed is not immune to port, connector and soldering losses. Moreover, the varying tolerance of the SMD again plays a role in shifting of resonant frequencies. To avoid this, one can fabricate multiple prototypes til the desired frequency is achieved. Another route that can be explored is using capacitors with extremely low tolerances.

### Section VII: Conclusion

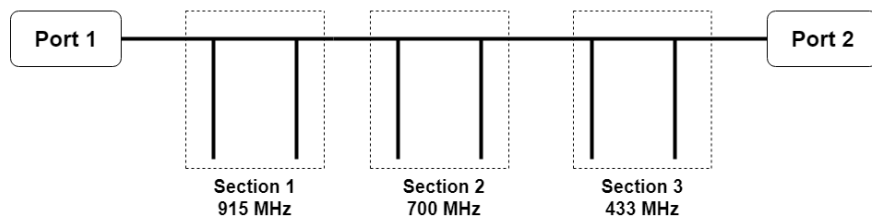
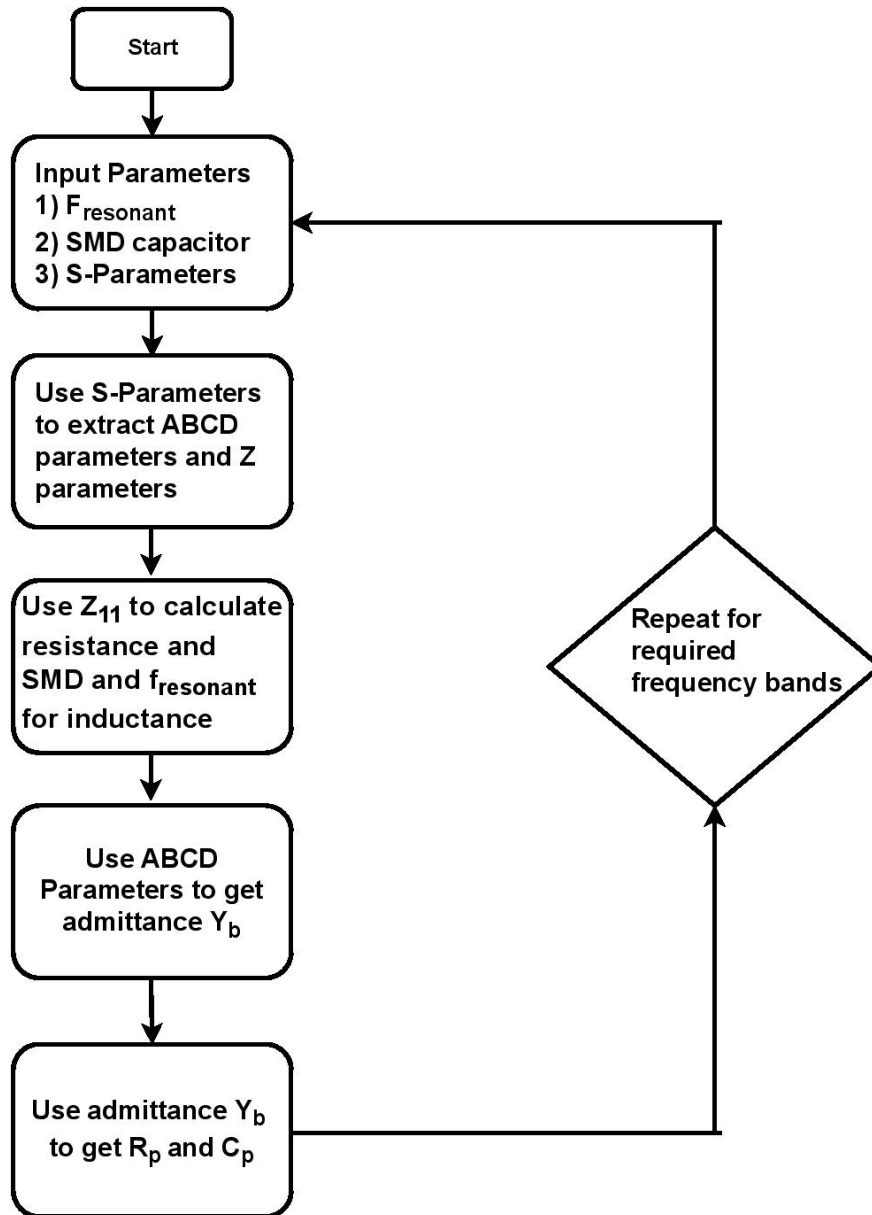
Two filters using Defected Ground Structures have been proposed in this paper. The first structure is single band BSF which has been extended to multiple bands by cascading multiple defects. This structure is then prototyped on a Rogers 4350B substrate of overall size 45 mm  $\times$  15 mm, and external SMD capacitors have been employed to control the resonance of the circuit, for the stopband frequencies of 433 MHz, 700 MHz and 915 MHz. An equivalent circuit is also proposed for this multi-band design. The second filter is a combination of a band-stop and band-pass filter in one structure. The filter, operating with a controllable passband and stopband frequency is fabricated, on Rogers 4350B lossy substrate, to validate the EM and circuit simulation results. Two SMD capacitors have been loaded in the filter to introduce a pass band frequency of 700 MHz and stop band frequency of 770 MHz, with an overall structure size of 20 mm  $\times$  20 mm. Finally, a novel equivalent circuit model encompassing the band-pass and band-stop frequency response of DGS based filters is proposed, which validates the EM and measured results.

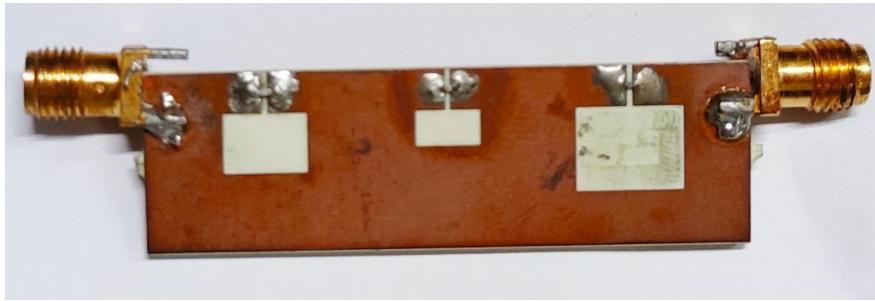
### References

1. Weng, Li Hong, et al. "An overview on defected ground structure." *Progress In Electromagnetics Research* 7 (2008): 173-189.
2. Tahar, F., et al. "1.06 FoM and compact wireless power transfer system using rectangular defected ground structure resonators." *IEEE Microwave and Wireless Components Letters* 27.11 (2017): 1025-102
3. Park, Jun-Seok, Jun-Sik Yun, and Dal Ahn. "A design of the novel coupled-line bandpass filter using defected ground structure with wide stopband performance." *IEEE Transactions on Microwave Theory and Techniques* 50.9 (2002): 2037-2043
4. Cao, Shihua, et al. "An ultra-wide stop-band LPF using asymmetric Pi-Shaped Koch fractal DGS." *IEEE Access* 5 (2017): 27126-27131.
5. Chen, Han-Jan, et al. "A novel cross-shape DGS applied to design ultra-wide stopband low-pass filters." *IEEE Microwave and Wireless Components Letters* 16.5 (2006): 252-254.
6. Chen, Han-Jan, et al. "A novel cross-shape DGS applied to design ultra-wide stopband low-pass filters." *IEEE Microwave and Wireless Components Letters* 16.5 (2006): 252-254.
7. Park, Jun-Seok, et al. "A novel equivalent circuit and modeling method for defected ground structure and its application to optimization of a DGS lowpass filter." *2002 IEEE MTT-S International Microwave Symposium Digest (Cat. No. 02CH37278)* . Vol. 1. IEEE, 2002.

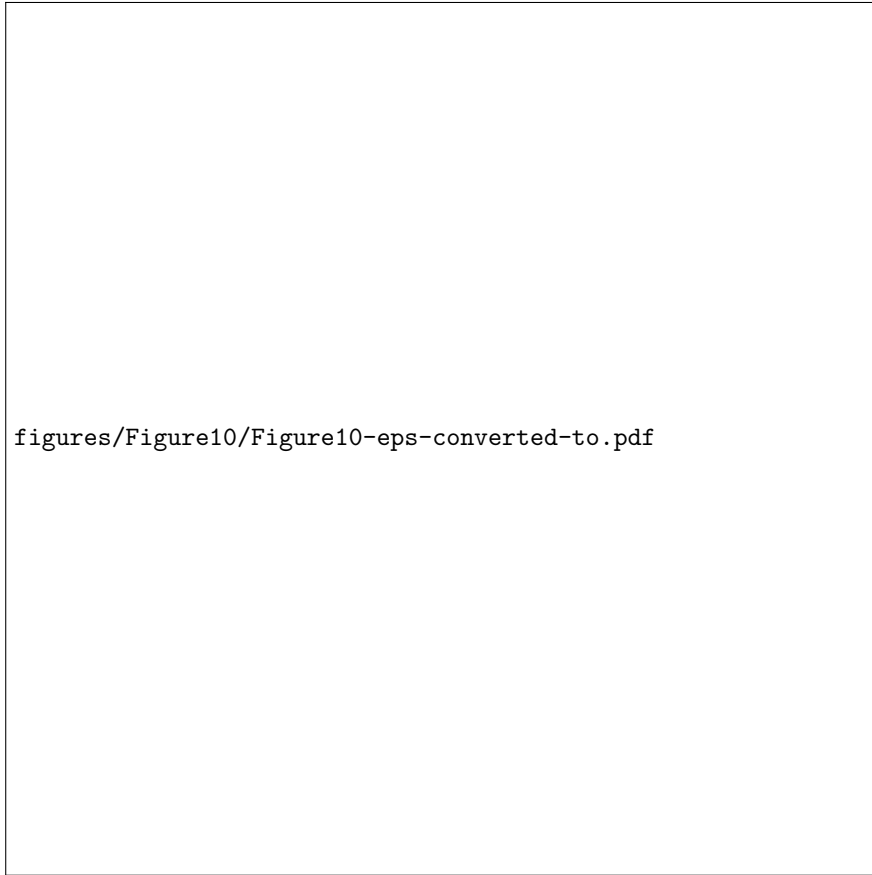


figures/Figure4/Figure4-eps-converted-to.pdf

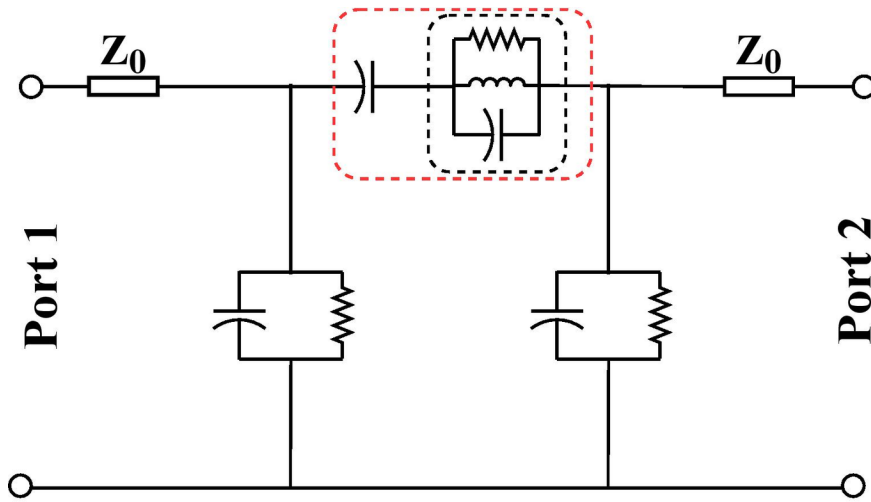
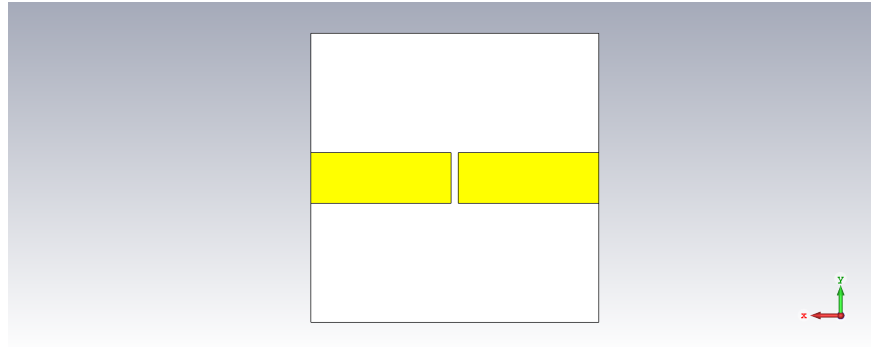
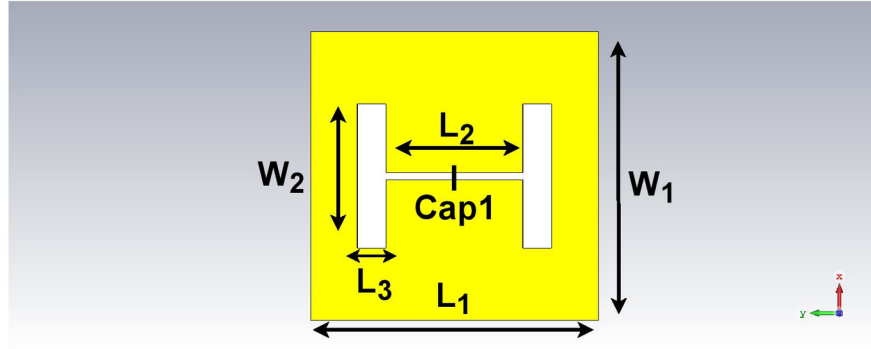




figures/Figure7/Figure7-eps-converted-to.pdf

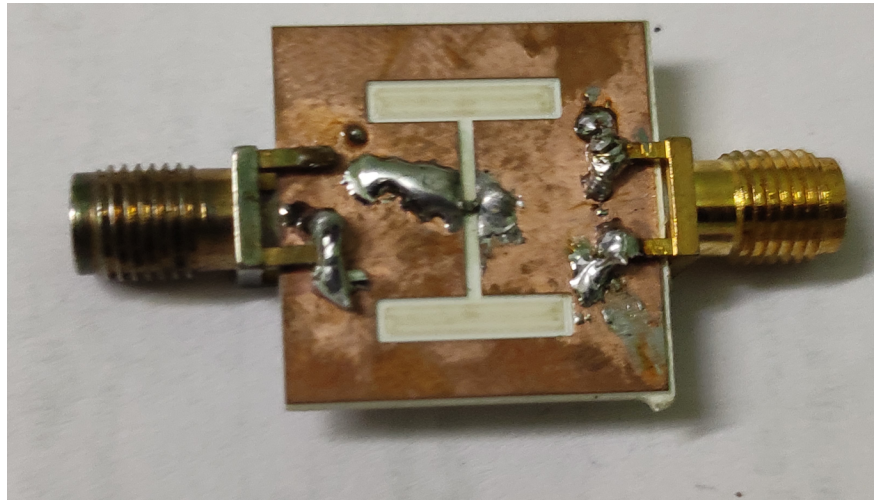


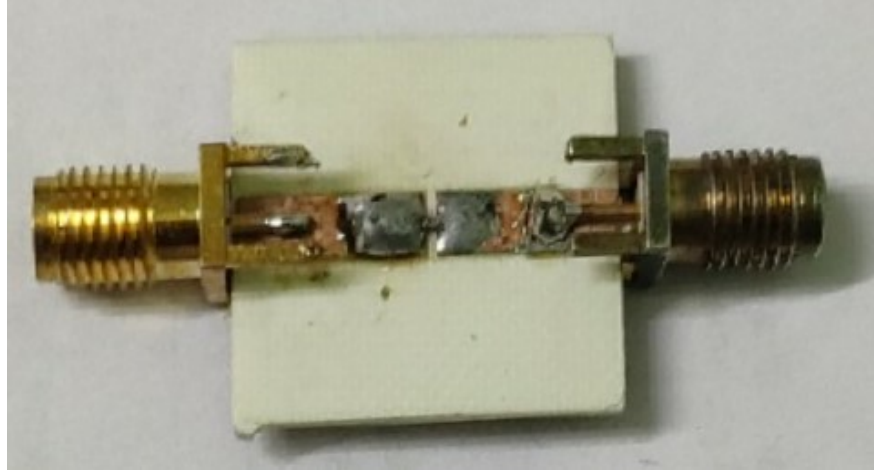
figures/figure10/figure10-eps-converted-to.pdf



Parallel Resonant-Bandstop  
 Series Resonance-Bandpass

figures/Figure14/Figure14-eps-converted-to.pdf





figures/Figure17/Figure17-eps-converted-to.pdf